Celal Bayar University Journal of Science

Relationship between microhardness and carbide in deep rolling of Al6061-T6 material with new type rolling insert

Oktay Adıyaman[1]*, Feyza Aydın[2]

[1] Beşiri Organized Industrial Zone Vocational School, Batman University, Türkiye
[2] Institute of Graduate Studies, Batman University, Türkiye
* oktay.adiyaman@batman.edu.tr
* Orcid No: 0000-0002-2674-3836

Received: March 22, 2025
Accepted: October 31, 2025
DOI: 10.18466/cbayarfbe.1663094

Abstract

Deep rolling is a surface modification technique based on the principle of rolling metal surfaces by plastic deformation with the help of a rolling insert tip. In this technique, different rolling tools, such as ball and roller, are used. In this study, a rolling tool compatible with existing tools was designed and used in deep rolling of Al6061-T6 alloy. The effect of the rolling tip used on the surface was examined and evaluated. For this purpose, three different rolling forces, feed rates, and spindle speeds were selected, and experiments based on the L27 orthogonal design were carried out for the rolling process. The surface hardness of the rolled surfaces was measured, and the effects of surface morphology and parameters on carbide mass on the surface were examined. As a result, it was observed that carbide was observed in deep rolling with the manufactured rolling insert tip, and thus, the microhardness increased. It was observed that carbide increases in parallel with the increase in spindle speed and rolling force and decreases with the increase in feed rate. It was also observed that the effects of the parameters on carbide mass are rolling force, spindle speed, and feed rate, respectively.

Keywords: Al6061, Ball burnishing, Deep rolling, Microhardness, Tribology

1. Introduction

Deep rolling method is a surface modification processing method used to correct the surface of metal parts after a process such as turning, milling, grinding, honing, lapping, ball rolling [1] or surface improvement by film coating with different materials [2]. The method first applied by Ford to axle shafts dates back to the 1930s [3]. In the method based on applying high pressure to the turned or ground surface with the help of a device with a rolling insert tip, very thin thickness stresses are formed on the surface after the process. Through this method, the micro peaks on the surface are subjected to plastic deformation by being rolled with the pressing tool and are compressed into micro valleys on the surface. The basic mechanics of this method is explained by the Hertzian theory [4] and is defined as the effect of the surface pressure created between the workpiece and the spherical ball tip in the contact area. As a result of the applied surface pressure, the yield strength of the material is exceeded, thus it causes residual stress on the surfaces and deformations (hardening or softening) in the microstructure [3, 5, 6]. Studies on deep rolling continue in many different ways, such as simulation of rolling[7], analysis with the finite element method [8, 9], testing the method in different working environments (e.g. cryogenic) [10], analysis of the method with regression methods [11], testing different rolling types [12, 13] and examining the effect of rolling tools on the results [14] etc. Results such as increased hardness, corrosion resistance and fatigue life improvement have been obtained with the compressive residual stress formed on the surfaces after deep rolling [15, 16, 17]. With this method, not only is good surface quality achieved, but also the propagation of the fatigue crack is delayed by residual compressive stresses [18]. With the effect of deep rolling from the surface to the section, values close to the depth values similar to nitriding, induction hardening and laser hardening processes are obtained [3]. Deep rolling process has been applied to Al and its alloys both on cylindrical surfaces by turning [19-25] and on planar surfaces by milling [26-28] and the results have been investigated. Deep rolling can be applied to soft materials such as Al as well as to hard metals such as Inconel steel [29]. Abrão et al. stated that the intensity of

plastic stress under the surface increased with the increase in rolling pressure and number of passes for AISI 1060 steel, and as a result, both the microhardness value and the depth of the affected area increased [30]. Loh et al. determined that the surface hardness of medium carbon steel increased by an average of 55% after deep rolling using tungsten carbide balls [31].

Deep rolling can cause the formation of dislocation cell structures [32], nanocrystals [33, 34], twinning or martensitic transformations [33] depending on the workpiece material type. When the surfaces from which microhardness values are taken are examined, it is seen that very different structures are formed within the same region.

The temperature generated in deep rolling is one of the most important criteria. Some studies have argued that the main source of formations on the surface is temperature [35, 8]. As a result of the surface undergoing plastic deformation (with changes in parameters such as feed rate, speed, etc.), temperature increases occur. In addition, with parameters such as high feed rate, more power (partially converted to heat in the ball-workpiece contact area) is required in deep rolling [8]. In addition, the increased heat caused by the wear mechanism causes the structure to transform from ferrite to structures such as pearlite or martensite. Accordingly, the increase in temperature is an important parameter of the work obtained in deep rolling. The temperature increases occurring on the part have an effect on increasing the work obtained thermodynamically. It has been stated that as a result of the heat remaining on the workpiece longer, phase transformations occur thermodynamically [36] and accordingly, hardness increases. Similar to this idea, [30, 35] found that partial annealing, full annealing or tempering occurred on the surface of carbon steels (AISI 1060) with the deep rolling process. In particular, it has been stated that the rolling pressure and the number of passes significantly increase the surface hardness [30]. On the other hand, as ferrite layers transform into pearlite during heat transfer, it has been observed in the studies that microhardness increases accordingly [36].

Another area of studies on deep rolling is the use and evaluation of different types of tools as rolling tools. In addition to the use of roller, ball, double roller rolling tools [12], the effect of the rolling tool dimensions was also investigated [37, 38]. It was observed that the best Ra values and hardness values were obtained with the ball type tool in the ball rolling of Al6061-T6 material with different tip types [12].

When all these studies are evaluated, no study has been found on the carbide formation, measurement and analysis of the process parameters used in deep rolling. In this study, the effect of the designed and manufactured deep rolling tool tip on the surface obtained in deep rolling was examined and its usability was investigated. The effect of the parameters on the carbon ratios was examined for each combination, and the use of the parameters on the % carbide ratio was also analyzed in pairs. It was discussed which parameter has the greatest effect, to what extent it affects and what are the ideal parameter values for obtaining the highest carbon ratio. The relationships between the obtained surface morphology and the parameters were also examined and analyzed. In this respect, it is aimed to open a new and different field for the studies on deep rolling in Al materials and to contribute to the literature by developing the subject.

2. Materials and Methods

As a result of the previous study conducted on the subject of this research [39, 40], it was determined that the rolling force was 495 N, the feed rate was 0.12 mm/rev and the spindle speed was 600 rpm as the most ideal parameter for the lowest surface roughness. It was also determined that the newly designed rolling tool was suitable for deep rolling operations and could be used in rolling operations on parts with conical, curved arcs and cylindrical surfaces. It was established that the most effective processing parameter on the Ra value was the feed rate value.

In this study, which is a continuation of previous studies [39, 40], SMARC brand CNC lathe was used for the application of experiments, turning and deep rolling operations. Due to the widespread use of the WNMG standard insert type in turning applications, this insert type was taken as a reference in the design and deep rolling tools were manufactured in the dimensions of this insert type. The inserts, whose design and manufacturing stages were completed, were connected to the MWLNR coded tool holders and the analyzes were completed by performing experiments. The experimental flow diagram related to the process is shown in Figure 1.

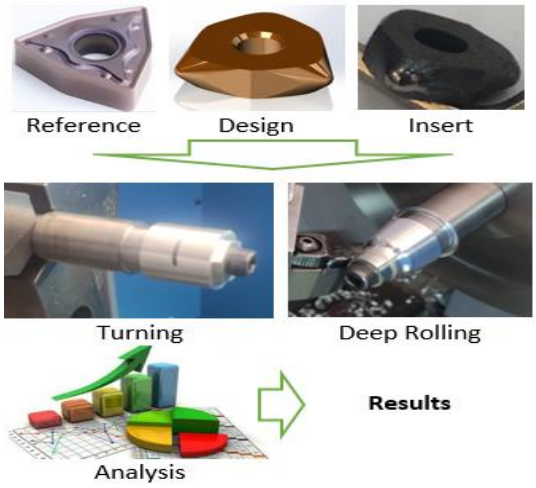

Figure 1. Process flow diagram

Celal Bayar University Journal of Science
Volume 22, Issue 1, 2026, p 21-31
Doi: 10.18466/cbayarfbe.1663094

The type of insert produced and shown in Figure 1 is attached to the tool holder and mounted on the CNC turret with the tool holder designed and manufactured to adjust the rolling force (Figure 2 a).

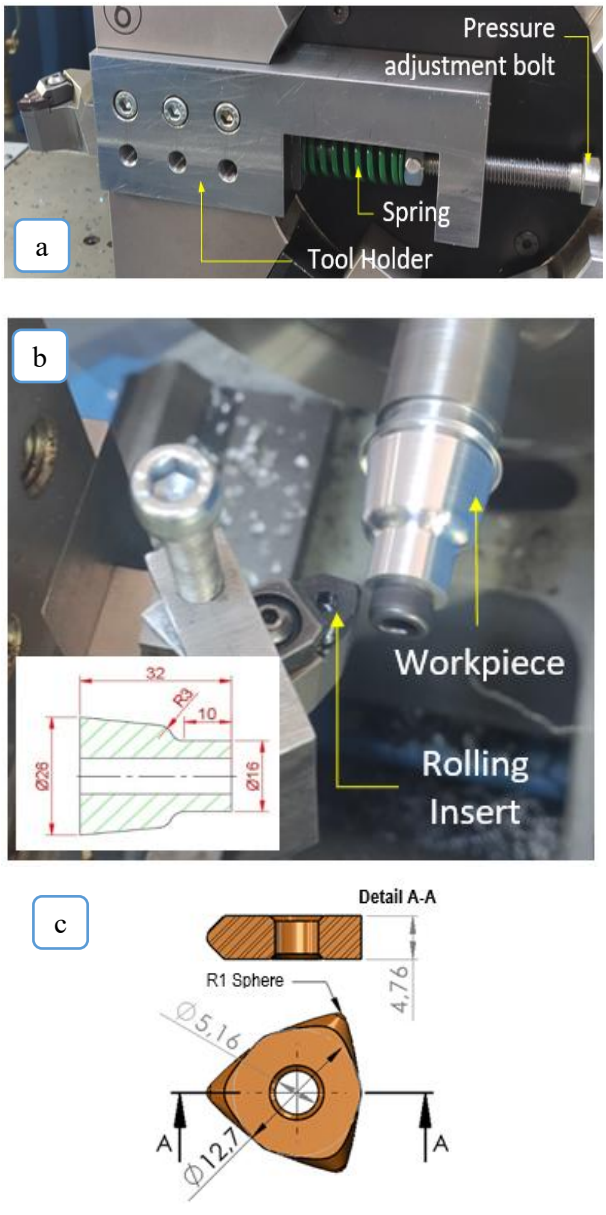

Figure 2. a) Connecting apparatus b) Technical drawing of the produced rolling tip c) Deep rolling process on the CNC lathe and workpiece technical drawing

The rolling force was adjusted by tightening the pressure adjustment spring length with the pressure adjustment bolt (Figure 2 a). The spring length and the pressure forces that can be obtained were determined by considering the company spring tables [41]. Here, rather than the precision of the rolling force, the application of three different rolling forces at the same level is taken as the basis. The technical drawing of the type of insert tip produced is shown in Figure 2 b, and the technical drawing of the deep rolled workpiece with the process is shown in Figure 2 c.

In deep rolling processes, Al 6061-T6 coded aluminum material was used as the material type for experimental applications. The chemical composition and mechanical properties of Al6061-T6 material are shown in Table 1.

Table 1. Chemical composition and mechanical properties of Al6061-T6

Chemical Content			
Elements			
Al	Remaining	Zn	0.25
Si	0.4-1.0	Cr	0.1
Cu	0.6-1.1	Fe	0.5
Mn	0.2-0.8	Ti	0.1
Mg	0.8-1.2	Other	0.15
Mechanical Properties			
Temper			T6
Yield Strength (MPa) min-max			240-270
Tensile Strength (MPa) min-max			260-310
Elongation (٪50) min-max			20
Hardness (brinel) min-max			95

In the experiments, Taguchi experimental design was preferred for experimental design and statistical analysis. In the experiments, L27 orthogonal array was used and combinations were created. A total of three parameters and accordingly 3 levels were determined for each parameter. Table 2 shows the rolling parameters in the deep rolling experiments.

Table 2. Process parameters and levels

Parameters	**Level 1**	**Level 2**	**Level 3**
Rolling Force (N)	143	330	495
Feed (mm/dev)	0.04	0.08	0.12
Rpm (rp/m)	400	600	800
Pass Number		1	
Rolling environment		Oil	

After using the rolling inserts in deep rolling, it is highly probable that there will be a diffusion transition from the rolling insert material to the main material due to the friction between the deep rolled workpiece and the rolling insert material. For this purpose, point and general SEM-EDX analyses were performed to determine the C element density on the surface of the main material (Figures 3 and 4). In the SEM images exhibited in Figures 3 and 4, it is seen that the pieces broken off from the roller end are embedded in the main material by diffusion as a result of the heat generated by friction. In light of the data obtained after the EDX analysis, it is determined that the C element transition from the rolling tool tip to the main material was intense when the table in Figure 4 is examined. It is observed that the C element formed in the main material was intensely at the particle level and embedded in the main material.

Celal Bayar University Journal of Science
Volume 22, Issue 1, 2026, p 21-31
Doi: 10.18466/cbayarfbe.1663094

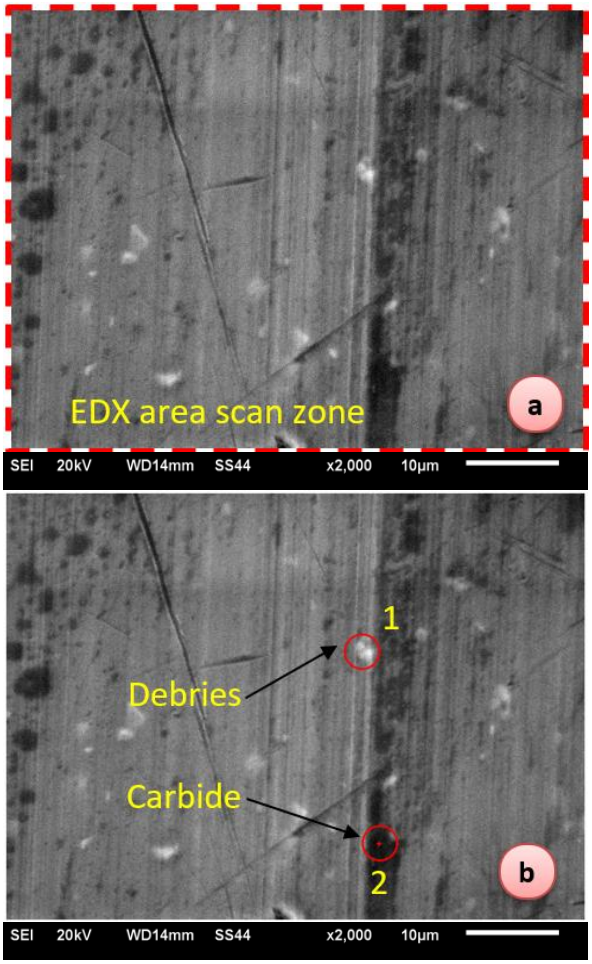

Figure 3. Exposures taken from samples in EDX analyses a) general mapping b) point regions

Considering the significant increase in the carbon element ratio, it can be considered that Al-based carbide phases are formed as stated in the literature. When compared with our EDX results in the Al-C phase diagram in Figure 5, they indicate Al and Al_4C_3 phases.

3. Results and Discussion

As seen in Table 1, there is no significant amount of C element in Al 6061-T6 material. However, the C element, which occurs as a result of the deep rolling process and is found in very little amount in the chemical composition of Al6061-T6 type aluminum (Table 1), can be formed as a result of friction and heat generation or diffusion and can form a hard layer on the surface. [45-47]. In other words, the friction results in an increase in heat. Aluminum reacts with the C element under high temperature to form aluminum carbide (Al_4C_3) or aluminum silicon carbide ($AlSiC_4$) [42]. In this case, two possibilities can be considered as the reason for the high C ratio. The first of these is that the very small amount of C element in the Al6061-T6 material and the C element in the roller insert form carbide phases on the surface with the heat generated by friction and thus affect the surface properties. For the second possibility, it is thought that the high C element ratio that occurs is caused by the diffusion from the rolling insert tool to the workpiece material.

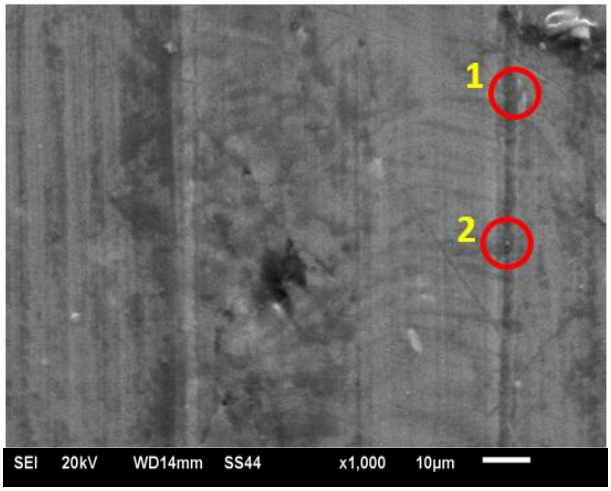

Element	General %C	Point 1 %	Point 2 %
B	0.000	0.000	0.000
C	5.605	8.844	6.592
F	0.047	0.000	0.000
Al	92.386	86.035	92.022
Si	0.544	4.078	0.306
P	0.010	0.014	0.024
S	0.000	0.042	0.000
Ca	0.035	0.054	0.039
Ti	0.058	0.068	0.040
Mn	0.255	0.170	0.199
Fe	0.251	0.089	0.109
Co	0.040	0.040	0.046
Ni	0,054	0.082	0.065
Zn	0.194	0.302	0.232
Mo	0.172	0.010	0.090
W	0.349	0.171	0.236

Figure 4. A sample taken for general and point mapping (17^{th} experiment)

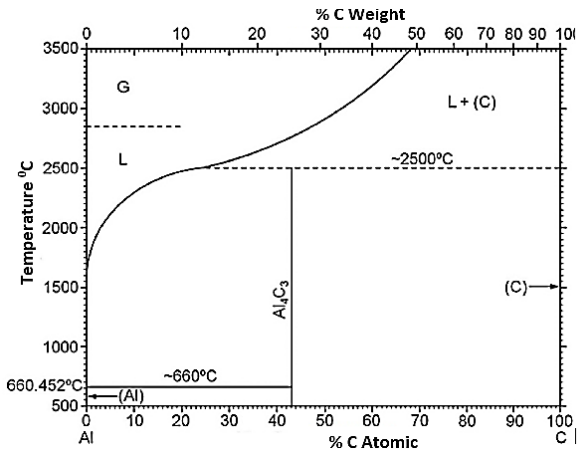

Figure 5. Al-C phase diagram [44]

Celal Bayar University Journal of Science
Volume 22, Issue 1, 2026, p 21-31
Doi: 10.18466/cbayarfbe.1663094

In this study, since the surface processing study was taken as the basis, phase transformations were not examined, SEM-EDX was performed only to determine whether there was a transition from the workpiece to the main material. In the SEM-EDX results, it is estimated from the carbon ratios in Figure 4 that there is a transition from the rolling insert to the main material, which contributes to the increase in the % C ratio on the surface. Depending on the C ratio, based on the phase diagram in Figure 5, it can be said that the possible carbide phases that occur within the structure contribute to the increase in microhardness. This result is already seen in the literature studies mentioned above. The EDX analysis and element ratios of the general mapping formed on the surface after deep rolling for all experiments are given in Table 3.

Table 3. C amount ratios and surface microhardness values according to experiments

Exp.No	Force (N)	Spindle (rpm)	Feed (mm/dev)	Microhardness (Hv_{30})	% C Ratio
1	143	400	0.04	158	0.034
2			0.08	163.53	0.045
3			0.12	165.26	0.018
4		600	0.04	154.8	0.088
5			0.08	164.1	0.098
6			0.12	169.6	0.076
7		800	0.04	162.73	3.099
8			0.08	163.7	4.264
9			0.12	158.76	2.124
10	330	400	0.04	164.46	2.285
11			0.08	173.26	2.21
12			0.12	164.86	2.123
13		600	0.04	151.8	7.86
14			0.08	165.66	5.45
15			0.12	158.63	2.99
16		800	0.04	167.13	7.47
17			0.08	155.9	5.605
18			0.12	160.7	3.82
19	495	400	0.04	168.1	4.05
20			0.08	159.53	3.2
21			0.12	161.46	3.79
22		600	0.04	165.4	11.48
23			0.08	174.7	5.756
24			0.12	164.96	5.88
25		800	0.04	162.63	10.211
26			0.08	156.86	5.927
27			0.12	157.5	5.91

When all the process parameters in Table 3 are examined, the relationship between the spindle speed and the C (carbon) rate at all three rolling forces (143N, 330N and 495N) is as shown in Figure 6.

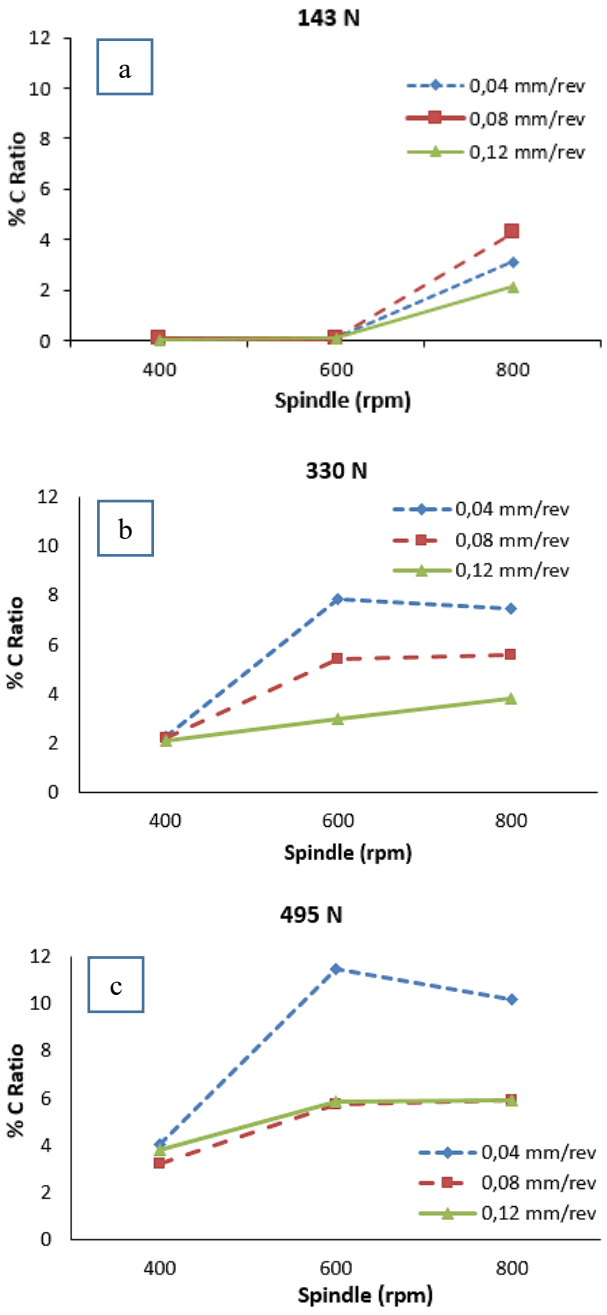

Figure 6. Relationship graph between % C ratio (carbide) and spindle speed a) 143 N b) 330 N c) 495 N

Here, when Figure 6 is examined, it is observed that the increase in % C ratios is directly proportional to the increase in rolling force. In addition, when Figure 6 a, b and c are examined together, it is determined that the same increase continues with the increase in the spindle speed. However, although this increase occurs with a significant difference between 400 rpm and 600 rpm, it is seen that in the range of 600-800 rpm and especially when 330 N (Figure 6 b) and 495 N (Figure 6 c) rolling force is applied, it is seen that close % C (carbon) ratios are formed in the horizontal trend. When the subject is considered in terms of feed rate, the highest % C amount is formed when the lowest feed rate is applied in all

Celal Bayar University Journal of Science
Volume 22, Issue 1, 2026, p 21-31
Doi: 10.18466/cbayarfbe.1663094

rolling force values. In addition, as seen in Figure 6 a, carbide is formed at high spindle speeds in deep rolling with low rolling force, and no carbide formation is observed on the surface at low spindle speeds. Considering this situation, it is thought that the % C ratio changes due to friction and temperature increase, and the increase in speed and temperature increases the % C ratio. It is thought that if the feed rate is small, the contact of the rolling insert with the surface of the part increases over time and, accordingly, the heat increase due to friction increases the % C ratio.

Considering the feed rate value in deep rolling, the graphs in Figure 7 were obtained in the analysis of the results of the % C ratio at the selected speeds.

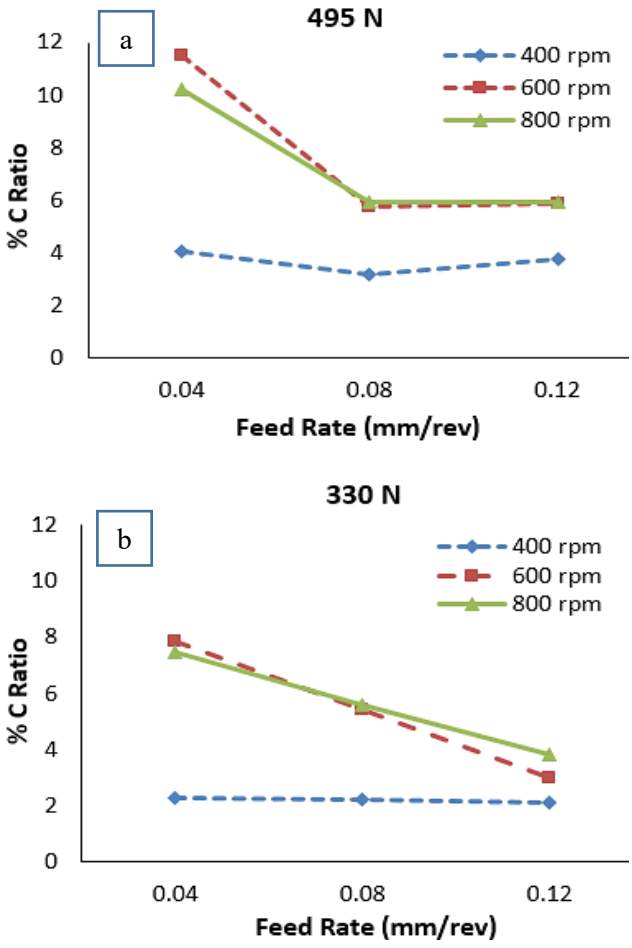

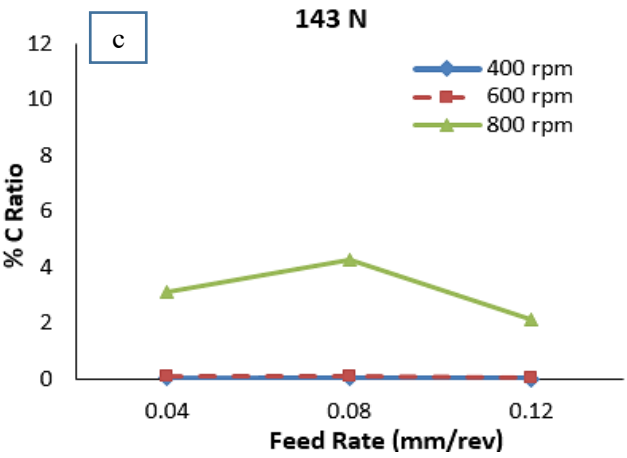

Figure 7. Relationship graph between % C ratio and feed rate a) 143 N b) 330 N c) 495 N

When the graphs in Figure 7 are examined, it is seen that the increase in feed rate at 400-600 rpm spindle speeds does not have any effect on the % C ratio at low rolling force values, but (Figure 7 a) an increase in the % C ratio is observed at 800 rpm spindle speed. However, it is also observed that the horizontal course does not change much despite the increase in feed rate. It is thought that this situation is due to the low rolling force of 143 N, the low plastic deformation on the surface of the material as a result of this value and the absence of major structural changes, and the resultant heat generated as a result of friction and wear mechanisms, and therefore, no increase in the % C ratio. At high rolling force values (330-495 N) (Figure 7 b and c), at low spindle speed (400 rpm), a horizontal trend is observed in the % C ratio with the increase in the feed rate, while at higher spindle speeds (600-800 rpm), it is observed that the increase in the feed rate causes a decrease in the % C ratio in an inversely proportional manner. When the highest rolling force is applied (495 N), it is observed that the % C ratios are formed in a way that they are close to each other at the feed values of 0.08-0.12 mm/rev. In addition, it is observed that the % C ratio increases with the increase in the rolling force as the spindle speed increases. Here, it is seen that low spindle speeds do not bring any change with the increase in feed (Figure 7 a). It is also seen that the % C ratio has a decreasing trend from low feed values to high feed values (Figure 7 b and c).

When the relationship between the rolling force and feed values of the process parameters is evaluated together, the graph in Figure 8 is obtained.

Celal Bayar University Journal of Science
Volume 22, Issue 1, 2026, p 21-31
Doi: 10.18466/cbayarfbe.1663094

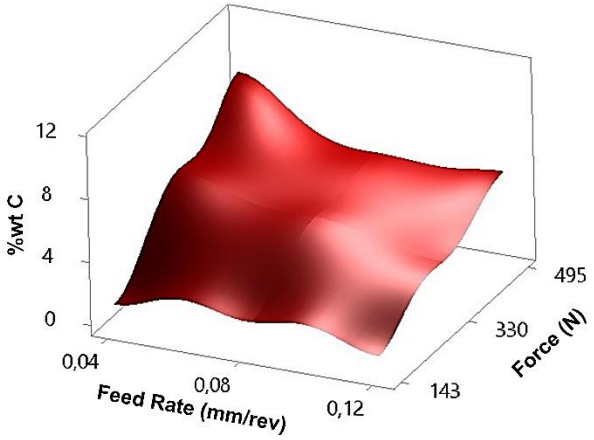

Figure 8. Interaction of rolling force and feed rate with % wt C.

When the Figure 8 graph is evaluated, it is seen that the lowest % C ratio occurs under conditions where the feed and rolling force are at their lowest. Here, as a basic principle, it can be stated that when the % C ratio is desired to be high, the feed values should be low and the rolling force should be increased. If the feed rate is selected at low values, the contact length at the insert-workpiece interface in deep rolling on the surface increases, and if the rolling force is selected at high values, it has an effect on the plastic deformation on the material surface in the sense that more material is forced. As a combination of both cases, it is thought that the % C ratio increases with the increase in the temperature in the material.

The relationship between rolling force and speed, which is another binary combination, is shown in the graph in Figure 9.

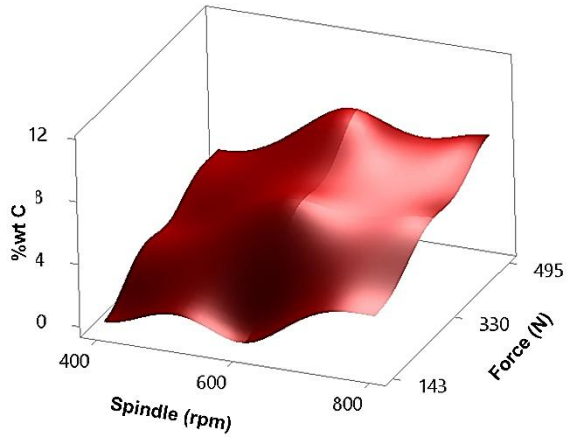

Figure 9. Interaction of rolling force and spindle speed with % wt C.

When the binary relationship graph in Figure 9 is evaluated, it is seen that there is an increase in the C % rate with the increase in the number of spindle speeds and the rolling force. Here, in parallel with the explanations above, the increase in the contact time on the deep rolled surface with the increase in the spindle speed and the increase in the amount of material that undergoes plastic deformation, the relative increase in temperature occurs due to the formation of more friction as a result of both increases, and thus the increase in the C % rate is thought to occur. When the relationship between the spindle speed and the progress is examined, the graph in Figure 10 is obtained.

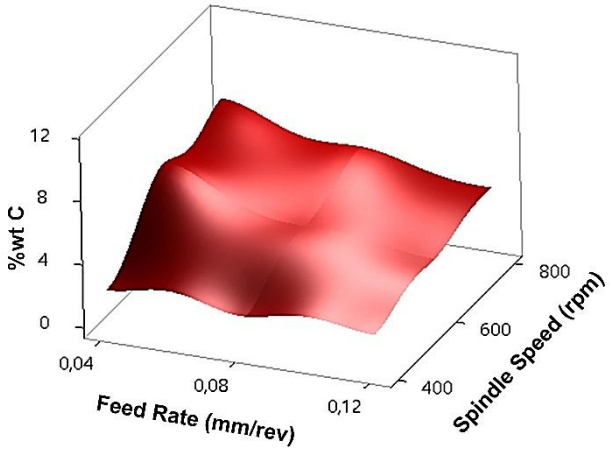

Figure 10. Interaction of feed and spindle speed relationship with % wt C.

When Figure 10 is examined, and when feed and spindle speed are considered together, it is seen that the % C ratio increases at low feed values and high spindle speeds. However, here, unlike other binary interactions, it is seen that there is a more horizontal relationship. Therefore, it can be concluded that in order to create the desired effect regarding the % C ratio, it will be more effective to make changes to other relationships.

Considering all the analyses performed, the graph in Figure 11 was obtained regarding the effect graphs of the parameters.

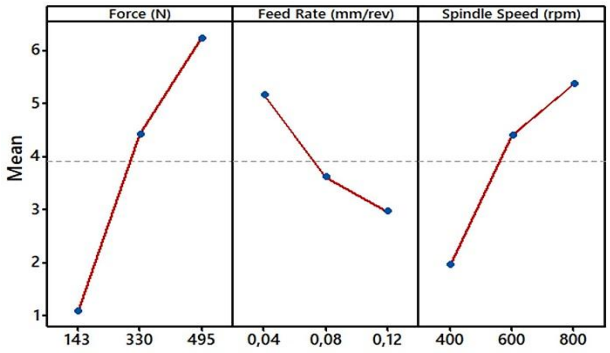

Figure 11. Effect graph of parameters

As can be seen from Figure 11, the greatest effect on the formation of % C is observed at the rolling force of 495

N, the feed rate of 0.04 mm/rev and the spindle speed of 800 rpm. In addition, while the same direction (directly proportional) effect is observed in the % C ratio with the increase in rolling force and spindle speed, a trend in the opposite direction is observed between the feed rate and the % C ratio.

As a result of examining the relationship between the C% ratio and process parameters, Variance Analysis (ANOVA) was performed to determine whether the parameters had an effect on the result and the amount of effect in percentage, and the results in Table 4 were obtained.

When Table 4 is examined, it is seen that the model has a high level of reliability at 80.92. In addition, it is seen that the significance levels (P Value) of all values in the variance analysis are lower than the coefficient of 0.05. This shows that all parameters have a significant effect on % C ratio. When the effect degrees of the parameters are examined, it is seen that the largest effect is in the rolling force with 49.34%, in the spindle speed with 22.29% and in the feed value with 9.29%, respectively. When the correlation between all parameters is examined, the data in Table 5 are obtained.

As seen in Table 5, while there is a strong relationship between C% ratio and the rolling force, this effect remains at a moderate level in the spindle speed. In the feed value, there is a correlation at the lowest value and in the opposite direction.

Table 5. Correlation between results and parameters

	%wt C	Force (N)	Feed Rate (mm/rpm)
Force (N)	0.722		
Feed Rate(mm/rev)	-0.296	0.000	
Spindle speed (rpm)	0.530	-0.000	0.000

Here, it is thought that the rolling tool provides more plastic deformation on the workpiece in direct proportion to the increase in rolling force and increases the temperature by increasing the friction force. It is thought that the increase in friction caused by the temperature increase and the diffusion of the tool into the material increased the carbide formation. Different studies that have obtained results such as partial annealing, full annealing or tempering on the surface support this [30, 35]. Similarly, with the increase in the spindle speed, the contact length of the tool on the workpiece per unit time increases, which causes more friction and friction wear, and an increase in temperature as well. This increases carbide formation again.

When looking at the feed rate value, the tool contact time and length decrease with the increase in feed rate, and the tool diffuses into the material in less time. Thus, a decrease in carbide formation occurs with the opposite effect. Maximov defines the obtained work (¯dA^e), the work converted into heat (dA_Q^e) and the work produced by the internal and external surface forces required for the elastic and plastic deformation of the workpiece, respectively (|dA_el |+|dA_pl |), except for the low-value environmental factors that do not have a great effect on the result in deep rolling (Equation 3.1) [36].

$$\overline{dA}^{e} = dA_{Q}^{e} + |dA_{el}| + |dA_{pl}| \quad \textbf{(3.1)}$$

As can be seen from the formula, the work obtained is defined as the work produced by elastic and plastic change. Since the work obtained is a time-dependent concept, the contact time and the amount of elastic and plastic deformation gain importance in deep rolling. It is seen that the increase in the rolling force affects the elastic and plastic deformation, and since the speed and feed values increase the time and the work produced accordingly, they affect the cumulative work obtained and cause an increase in heat. The increase in heat also causes carbide formation.

Table 4. Variance (ANOVA) analysis on % wt C

The Summary of the Model

S	R-sq	R-sq(adj)	PRESS	R-sq(pred)
1.54110	80.392%	75.19%	86.5687	65.22%

Variance Analysis

Source	DF	Seq SS	Impact Value	Adj SS	Adj MS	F-Value	P-Value
Force (N)	2	122.81	49.34%	122.81	61.403	25.85	0.000
Feed (mm/rev)	2	23.13	9.29%	23.13	11.563	4.87	0.019
Spindle speed (rpm)	2	55.49	22.29%	55.49	27.744	11.68	0.000
Error	20	47.50	19.08%	47.50	2.375		
Total	26	248.92	100.00%				

4. Conclusion and Suggestions

The following conclusions were reached based on the examination of the carbide formation on the surface as a result of the deep rolling process performed with the rolling insert designed and manufactured for the deep rolling of Al6061-T6 material and the analyses made between the parameters and the carbide ratio:

- The images of the surfaces obtained as a result of deep rolling were taken with an optical microscope at 200x magnification
- In the images, it was seen that the structure was homogeneously distributed in these images.
- EDX analyzes of the deep rolled surfaces were performed and it was seen that the highest elemental change on the surfaces was in the % C (carbon) ratio.
- It was seen that the feed rate and % C ratio values were inversely proportional and the highest % C ratio values were obtained at the lowest feed rates.
- It was seen that there was a direct proportion between the rolling force and the number of revolutions in terms of the obtained % C ratio values
- It was seen that the % C ratio increased with the increase in the rolling force and number of revolutions.
- The temperature increase increases the % C ratio due to the increase in the pressure on the material undergoing plastic deformation together with the increase in the contact length of the increase in the number of revolutions and rolling force.
- It is seen that the model obtained with the variance analysis has a high level of reliability at a value of 80.92.
- It is seen that all values in the variance analysis have a significant effect on carbide formation.
- The effect degrees of the process parameters in deep rolling on carbon diffusion were found to be rolling force with 49.34%, spindle speed with 22.29% and feed rate with 9.29%, respectively.
- It was found that rolling force and spindle speed were directly proportional and positively affected, while feed rate was inversely proportional and negatively affected.

The following suggestions can be given for further studies on deep rolling of Al6061-T6 material:

- In order to obtain lower Ra values, research can be conducted on the application and comparison of deep rolling process in oily and oil-free environments.
- More intensive studies are needed on the examination of surface and subsurface structure with XRD analyses and SEM analyses, detection of phase transformations (especially phases such as aluminum carbide (Al_4C_3) and aluminum silicon carbide ($AlSiC_4$)), and interaction with the subsurface.

Acknowledgement

In order to carry out the research, Batman University unit of BAP (Scientific Research Projects) provided financial support to this study numbered BTUBAP-2022-YL-05.

Author's Contributions

Oktay Adıyaman: Conducted the experiment and result analysis, and then drafted and prepared the article.

Feyza Aydın: Assisted and supervised the study, as well as helped in manuscript preparation.

Ethics

There are no ethical issues after the publication of this manuscript.

References

[1]. Yılmaz, S, S, Ünlü, B, S, Varol, R. (2008). Borlama ve Bilyalı Dövmenin Demir Esaslı T/M Malzemelerde Aşınma ve Mikro Yapı Özelliklerine Etkisi. Celal Bayar University Journal of Science; 4(1): 1-8.

[2]. Aksu, P. (2024). Investigation of Thickness Effect on Structural and Magnetic Properties of Ni Thin Films for Some Applications. Celal Bayar University Journal of Science; 20(3): 19-24.

[3]. Altenberger, I., Scholtes, B. (2000). Recent developments in mechanical surface optimization. In Materials science forum, Trans Tech Publications Ltd; 347: 382-398.

[4]. Broszeit, E. (1984). Grundlagen der Schwingfestigkeitssteigerung durch Fest-und Glattwalzen. Materialwissenschaft und Werkstofftechnik; 15(12): 416-420.

[5]. Altenberger, I. (2003). Alternative mechanical surface treatments: microstructures, residual stresses & fatigue behavior. Shot Peening; 419-434.

[6]. Berstein, G., Fuchsbauer, B. (1982). Deep rolling and fatigue strength. Z. Werkstofftech; 13(3): 103-109.

[7]. Maiß, O., Röttger, K. (2022). Monitoring the surface quality for various deep rolling processes–limits and experimental results, Procedia CIRP; 108: 857-862. (https://doi.org/10.1016/j.procir.2022.05.199)

[8]. Kinner-Becker, T., Zmich, R., Sölter, J., Meyer, D. (2021). Combined laser and deep rolling process as a means to study thermo-mechanical processes. Procedia CIRP; 102: 369-374, 2021, (https://doi.org/10.1016/j.procir.2021.09.063)

[9]. Oevermann, T., Wegener, T., Liehr, A., Hübner, L., Niendorf, T. (2021). Evolution of residual stress, microstructure and cyclic performance of the equiatomic high-entropy alloy CoCrFeMnNi after deep rolling. International Journal of Fatigue; 153: 106513. (https://doi.org/10.1016/j.ijfatigue.2021.106513)

[10]. Martins, A. M. Leal, C. A. Campidelli, A. F. Abrão, A. M. Rodrigues, P. C. Magalhães, F. C. Meyer, K. (2022). Assessment of the temperature distribution in deep rolling of hardened AISI 4140 steel. Journal of Manufacturing Processes; 73: 686-694, 2022. (https://doi.org/10.1016/j.jmapro.2021.11.052)

[11]. Prabhu, P. R., Kulkarni, S. M., Sharma, S. S. (2011). An experimental investigation on the effect of deep cold rolling parameters

on surface roughness and hardness of AISI 4140 steel. World Academy of Science, Engineering and Technology; 60: 1594-1598.

[12]. Başak, H, Sönmez, F. (2015). Haddeleme İşleminde Haddeleme Aparat Tipinin Bilyeli Makaralı Çift Makaralı Yüzey Pürüzlülüğü ve Yüzey Sertliğine Etkilerinin İncelenmesi. Politeknik Dergisi; 18(3): 125–132.

[13]. Adıyaman, O, Aydın, F. (2024). Deep Rolling of Al6061-T6 Material and Performance Evaluation with New Type Designed WNMG Formed Rolling Tool. Celal Bayar University Journal of Science; 20(1): 29-40.

[14]. Başak, H, Sönmez, F. (2017). Examination of the Effects of Burnishing Apparatus on Surface Roughness and Hardness in Burnishing Process, Indian Journal of Engineering And Materials Sciences; 24(2) 115–122.

[15]. Altenberger, I. Deep rolling–the past, the present and the future. In Conf Proc: ICSP, France, (2005), 9, pp. 144-155.

[16]. Nalla, R. K., Altenberger, I., Noster, U., Liu, G. Y., Scholtes, B., Ritchie, R. O. (2003). On the influence of mechanical surface treatments—deep rolling and laser shock peening—on the fatigue behavior of Ti–6Al–4V at ambient and elevated temperatures. Materials Science and Engineering: A; 355(1-2): 216-230.

[17]. Noster, U., Altenberger, I., Scholtes, B. (2001). Combined mechanical and thermal surface treatment of magnesium wrought alloy AZ31. WIT Transactions on Engineering Sciences; 33.

[18]. Scholtes, B., (1997). Assessment of residual stresses, Structural and residual stress analysis by non-destructive methods V. Hauk, Ed., Elsevier; 590–632.

[19]. El-Axir, M.H., El-Khabeery, M.M. (2003). Influence of orthogonal burnishing parameters on surface characteristics for various materials. Journal of Materials Processing Technology; 132: 82–89, 2003.
(https://doi.org/10.1016/S0924-0136(02)00269-8)

[20]. Hassan A.M. (1997). An Investigation into the surface characteristics of burnished cast Al-Cu Alloys. International Journal of Machine Tools & Manufacture; 37(6): 813-821.

[21]. Hassan A. D., Maqableh A. M. (2000). The effects of initial burnishing parameters on non-ferrous components. Journal of Materials Processing Technology; 102 (1-3): 115-121.
(https://doi.org/10.1016/S0924-0136(00)00464-7)

[22]. Luo H., Wang L., Zhang C. (2011). Study on the aluminum alloy burnishing processing and the existence of the outstripping phenomenon. Journal of Materials Processing Technology; 116: 88-90.

[23]. Majzoobi, G.H. Jouneghani, F.Z., Khademi, E. (2016). Experimental and numerical studies on the effect of deep rolling on bending fretting fatigue resistance of Al7075. Int. J. Adv. Manuf. Technol*;* 82: 2137–2148.
(https://doi.org/10.1007/s00170-015-7542-z)

[24]. Yu X., Wang L. (1999). Effect of various parameters on the surface roughness of an aluminium alloy burnished with a spherical surfaced polycrystalline diamond tool. International Journal of Machine Tools & Manufacture; 39(3): 459–469.
(https://doi.org/10.1016/S0890-6955(98)00033-9)

[25]. Zhuang, W., Liu, Q., Djugum, R., Sharp, P.K., Paradowska, A. (2014). Deep surface rolling for fatigue life enhancement of laser clad aircraft aluminium alloy. Applied Surface. Science; 320: 558–562, 2014.
(https://doi.org/10.1016/ j.apsusc.2014.09.139)

[26]. Başak H., Goktaş H.H. (2009). Burnishing process on Al-alloy and optimization of surface roughness and surface hardness by fuzzy logic. Materials and Design; 30: 1275–1281.
(https://doi.org/10.1016/j.matdes.2008. 06.063)

[27]. Khabeery M. M., Axir M. H. (2001). Experimental techniques for studying the effects of milling roller-burnishing parameters on surface integrity. International Journal of Machine Tools&Manufacture*;* 41(12): 1705–1719.
(https://doi.org/10.1016/S0890-6955(01)00036-0)

[28]. Tadic B., Todorovic M. P., Luzanin O., Miljanic D., Jeremic M. B., Bogdanovic B., Vukelic D. (2013). Using specially designed high-stiffness burnishing tool to achieve high-quality surface finish. The International Journal of Advanced Manufacturing Technology; 67: 601–611.
(https://doi.org/10.1007/s00170-012-4508-2)

[29]. Çelik, M. (2023). Ezerek Parlatma Yönteminin Inconel 718 alaşiminin yüzey kalitesi üzerindeki etkilerinin araştirilmasi. Fırat Üniversitesi Mühendislik Bilimleri Dergisi; 35(1): 333-342.
(https://doi.org/10.35234/fumbd.1229068)

[30]. Abrão, A.M.; Denkena, B.; Köhler, J.; Breidenstein, B.; Mörke, T. (2014). The influence of deep rolling on the surface integrity of AISI 1060 high carbon steel. Procedia CIRP; 13, 31–36.
(https://doi.org/10.1016/j.procir.2014.04.006)

[31]. Loh, N. H., Tam, S. C., Miyazawa, S. (1998). A study of the effects of ballburnishing parameters on surface roughness using factorial design. Journal of Mechanical Working Technology; 18(1): 53-61.

[32]. Altenberger, I., Scholtes, B., Martin, U., Oettel, H. (1998). Mikrostruktur und Wechselverformungs verhalten des mechanisch randschichtverfestigten Stahls Ck 45. HTM. Härterei-technische Mitteilungen; 53(6): 395-406.

[33]. Altenberger, I., Scholtes, B., Martin, U., Oettel, H. (1999). Cyclic deformation and near surface microstructures of shot peened or deep rolled austenitic stainless steel AISI 304. Materials Science and Engineering: A; 264(1-2): 1-16.

[34]. Altenberger, I., Nalla, R. K., Noster, U., Liu, G., Scholtes, B. (2003). Verhalten laserschockverfestigter und festgewalzter Randschichten der Ti-Legierung Ti-6Al-4V bei schwingender Beanspruchung unter erhöhten Temperaturen. Materialwissenschaft und Werkstofftechnik: Entwicklung, Fertigung, Prüfung. Eigenschaften und Anwendungen technischer Werkstoffe; 34(6): 529-541.

[35]. Abrão, A.M., Denkena, B., Koehler, J., Breidenstein, B., Moerke, T. (2015). The inducement of residual stress through deep rolling of AISI 1060 steel and its subsequent relaxation under cyclic loading. Int. J. Adv. Manuf. Technol; 79: 1939–1947.
(https://doi.org/10.1007/s00170-015-6946-0)

[36]. Maximov, J. T. Duncheva, G. V. Anchev, A. P. Dunchev, V. P. (2020). Slide burnishing versus deep rolling-a comparative analysis. The International Journal of Advanced Manufacturing Technology; 110(7): 1923-1939.
(https://doi.org/10.1007/s00170-020-05950-2)

[37]. Başak, H. (2015). Haddeleme (Galetaj) ile 5083 Al-Mg malzeme yüzeyinin işlenmesi, haddeleme parametrelerinin yüzey pürüzlülüğü ve yüzey sertliğine etkilerinin incelenmesi. Gazi Üniversitesi Fen Bilimleri Dergisi; 3(2): 471-476.

[38]. Başoğlu, F., Kurgan, N. (2019). Temper haddelemede merdane parametrelerinin ERD6112 kalite sac malzemelerin pürüzlülük transferine etkisinin deneysel incelenmesi. Bilecik Şeyh Edebali Üniversitesi BŞEÜ Fen Bilimleri Dergisi; 6 (2): 344-356.

[39]. Aydın, F., Adıyaman, O. (2023). Experimental ınvestigation of new type ınsert in deep rolling of Al6061-T6 material. Rahva Journal of Technical and Social Studies; 3(1): 58-72.

[40]. Aydın, F., Adıyaman, O., (2023). Yeni tip ınsert uç ile Al6061 malzemeye bilyeli parlatma yöntemi uygulanması ve yüzey özelliklerinin incelenmesi. 2nd International Rahva Technical and Social Researches Congress, Bitlis, Türkiye.

[41]. Yüce Teknik. https://www.yuceteknik.com/Mekanik-Kalip-Yaylari-Yesil-Yay,PR-1779.html (accessed a: 27/09/2023).

[42]. Kalemtaş, A., & Arslan, G. (2009). Silisyum karbür-alüminyum karma yapilarinda alüminyum karbür oluşumunun taramali elektron mikroskobu ile incelenmesi. Anadolu Üniversitesi Bilim ve Teknoloji Dergisi; 10(1): 249-257.

[43]. Ohtani, H., Yamano, M., Hasebe, M., (2004). Thermodynamic Analysis of the Fe-Al-C Ternary System by Incorporating ab initio Energetic Calculations into the CALPHAD Approach. ISIJ International; 44: 1738–1747. (https://doi.org/10.2355/isijinternational.44.1738)

[44]. Dabouz, R., Bendoumia, M., Belaid, L., Azzaz, M. (2019). Dissolution of Al 6% wt C Mixture Using Mechanical Alloying. In Defect and Diffusion Forum, Trans Tech Publications Ltd.; 391, 82-87.

[45]. Dabade, U. A., Jadhav, M. R. (2016). Experimental study of surface integrity of Al/SiC particulate metal–matrix composites in hot machining. Procedia Cirp; 41: 914-919.

[46]. Li, J., Zhang, G., Liu, D., Ostrovski, O. (2011). Low-temperature synthesis of aluminium carbide. ISIJ international; 51(6): 870-877.

[47]. Ozcatalbas, Y. (2003). Investigation of the machinability behaviour of Al_4C_3 reinforced Al-based composite produced by mechanical alloying technique. Composites Science and Technology; 63(1): 53–61.